JACS
JOURNAL OF THE AMERICAN CHEMICAL SOCIETY
Article
pubs.acs.org/JACS

Rhodium-Coordinated Poly(arylene-ethynylene)-*alt*-Poly(arylene-vinylene) Copolymer Acting as Photocatalyst for Visible-Light-Powered NAD^+/NADH Reduction

Kerstin T. Oppelt,*[,†] Jacek Gasiorowski,[‡,⊥] Daniel Ayuk Mbi Egbe,[‡] Jan Philipp Kollender,[§] Markus Himmelsbach,[∥] Achim Walter Hassel,[§] Niyazi Serdar Sariciftci,[‡] and Günther Knör[†]

[†]Institute of Inorganic Chemistry, Johannes Kepler University Linz, Altenberger Strasse 69, 4040 Linz, Austria

[‡]Linz Institute of Organic Solar Cells (LIOS), Physical Chemistry, Johannes Kepler University Linz, Altenberger Strasse 69, 4040 Linz, Austria

[⊥]Semiconductor Physics, Technical University of Chemnitz, Reichenhainer Strasse 70, 09126 Chemnitz, Germany

[§]Institute of Chemical Technology of Inorganic Materials (ICTAS), Johannes Kepler University Linz, Altenberger Strasse 69, 4040 Linz, Austria

[∥]Institute of Analytical Chemistry (IAC), Johannes Kepler University Linz, Altenberger Strasse 69, 4040 Linz, Austria

Supporting Information

ABSTRACT: A 2,2′-bipyridyl-containing poly(arylene-ethynylene)-*alt*-poly(arylene-vinylene) polymer, acting as a light-harvesting ligand system, was synthesized and coupled to an organometallic rhodium complex designed for photocatalytic NAD^+/NADH reduction. The material, which absorbs over a wide spectral range, was characterized by using various analytical techniques, confirming its chemical structure and properties. The dielectric function of the material was determined from spectroscopic ellipsometry measurements. Photocatalytic reduction of nucleotide redox cofactors under visible light irradiation (390−650 nm) was performed and is discussed in detail. The new metal-containing polymer can be used to cover large surface areas (e.g. glass beads) and, due to this immobilization step, can be easily separated from the reaction solution after photolysis. Because of its high stability, the polymer-based catalyst system can be repeatedly used under different reaction conditions for (photo)chemical reduction of NAD^+. With this concept, enzymatic, photo-biocatalytic systems for solar energy conversion can be facilitated, and the precious metal catalyst can be recycled.

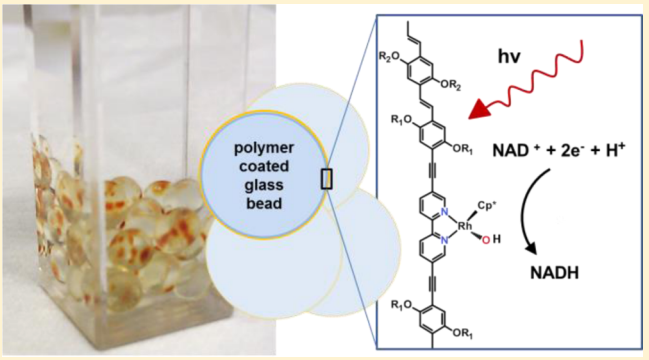

INTRODUCTION

In the field of artificial photosynthesis, the coupling of photocatalytic and enzymatic processes has recently gained increasing attention.[1−3] One possible merging point is the combination of photocatalytic cofactor reduction steps with enzymatic carbon dioxide reduction.[4−7] Here, the two fields of photoenzymatic CO_2 reduction and classical biocatalysis meet similar needs. Recycling of two-electron-reduced compounds, such as the reduced form of nicotinamide adenine dinucleotide (NADH) or flavin cofactors, is a widely applied strategy that saves valuable resources. In the presence of electron-donating substrates, NADH regeneration can be achieved either biochemically, using different oxidoreductase enzymes, or via chemical catalysis[8−11] and artificial photosynthetic reaction centers.[12] In response to increasing interest in sustainable CO_2 fixation based on renewable energy research, visible-light-driven cofactor conversion systems have been suggested for photoenzymatic CO_2 reduction.[6,12] The goal of such processes is to couple the photocatalyzed recycling of nicotinamide adenine dinucleotide (NAD^+) to biocatalytic transformations of CO_2 or carbonates with a cascade of enzymes producing formates, formaldehyde, and/or methanol,[8−11,13] which can be considered as carbon-neutral solar fuels.[14,15]

Photoenzymatic reactions require light-harvesting chromophores efficiently interacting with the functional components responsible for catalysis.[1−3,16] In this context, metal-binding and visible-light-absorbing polymeric compounds with a bis-5,5′-(phenylene-ethynylene)-2,2′-bipyridylene backbone represent quite interesting building blocks for the development of novel photocatalytic systems, as they provide the possibility of tuning the optical properties of the polymer-based ligand as well as the catalytic and optical properties of the coordinated metal complexes.[15,17−21]

Received: June 17, 2014
Published: August 18, 2014

   dx.doi.org/10.1021/ja506060u | J. Am. Chem. Soc. 2014, 136, 12721−12729

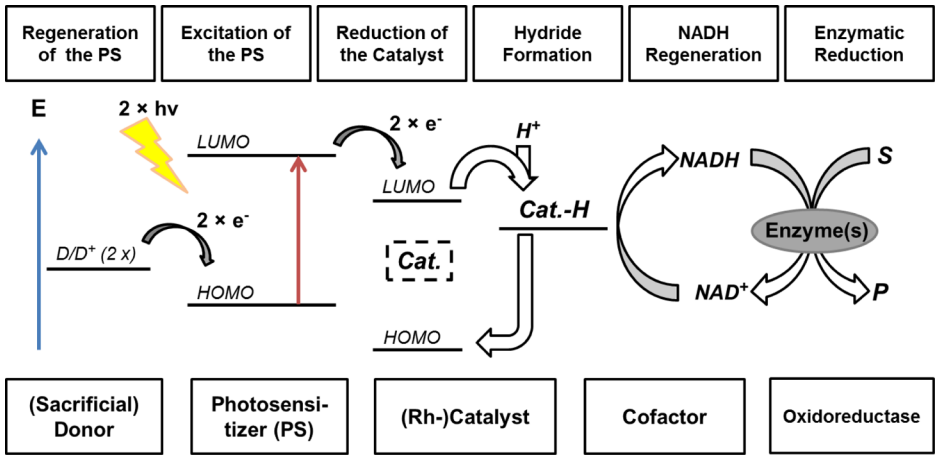

Figure 1. Schematic energy diagram and reaction pathway of the photochemical reduction of NADH with coupled enzymatic processes: D, donor; PS, photosensitizer; Cat., hydrogenation catalyst-oxidized form; Cat.-H, hydrogenation catalyst-active hydride species; S, substrate; P, product.

Scheme 1. Synthesis of the Bipyridine-Containing Polymer BipyE-PV*ab*

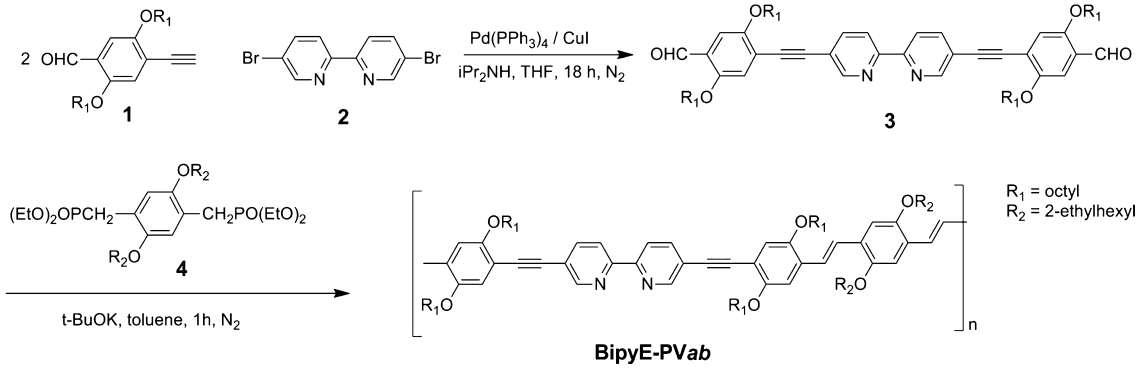

Different rhenium bis-5,5′-(phenylene-ethynylene)-2,2′-bipyridylene complexes, for example, were thoroughly investigated by Schanze and co-workers.[20,21] Ruthenium-containing polymers incorporating 4,4′- or 5,5′-(phenylene-ethynylene)-2,2′-bipyridylene moieties as ligands have been introduced and widely characterized by Klemm et al. as well as other groups.[18,22,23] In earlier studies we investigated both spectroscopic[24] and catalytic properties of bis-5,5′-(phenylene-ethynylene)-2,2′-bipyridylene-based oligomeric and polymeric rhenium and rhodium compounds. The rhodium η^5-cyclopentadienyl half-sandwich complex of bis-5,5′-(phenyl-ethynylene)-2,2′-bipyridine was successfully applied on a redox-active electrode for the regeneration of NAD^+ to NADH.[15]

It is well established that organometallic rhodium complexes of the type $[RhCp^*(1,2\text{-diimine})H_2O]^{2+}$ (with 1,2-diimine being derivatives of 2,2′-bipyridine (bpy) or 1,10-phenanthroline; Cp* = pentamethyl-cyclopentadienyl) accelerate the formation of NADH in neutral to slightly basic aqueous solutions. They have been investigated for chemical,[9,10] photochemical,[12,25−32] and electrocatalytic[10,33,34] cofactor reduction of NADH and model compounds.[27,35−37] These rhodium diimine complexes exhibit favorable catalytic properties, e.g., good selectivity in the hydrogenation of NAD^+ to form the enzymatically active 1,4-dihydronicotinamide isomer of NADH in addition to high reaction rates for the reduction reaction.[35−38] Efforts were also made to immobilize $[RhCp^*(diimine)H_2O]^{2+}$ as electrocatalysts. Work in this direction has been published by Cosnier et al.,[39,40] who electropolymerized a pyrrole-substituted bipyridyl-rhodium complex and applied this electrode to electrochemical cofactor reduction. Light-driven regeneration reactions of the NADH cofactor in various systems are also, with few exceptions,[4,5,41] often based on $[RhCp^*(bpy)H_2O]^{2+}$ as hydride-transfer catalyst. They are combined with different molecular and heterogeneous photosensitizers, e.g., rhodamine dyes,[25,32] semiconducting particles and quantum dots,[42,43] metalloporphyrins,[12,29] and, quite recently, graphene-derived photosensitizers.[44] In the field of heterogeneous photosensitizing agents, structured carbon nitride materials have recently shown promising performance as photosensitizers for $[RhCp^*(bpy)H_2O]^{2+}$ in selective 1,4-NADH regeneration. These surface-engineered carbon nitride materials can also reduce NAD^+ without use of a redox mediator; however, this leads also to the formation of enzymatically inactive 1,6-dihydronicotinamide isomer.[45−48] It seems thus advantageous to keep the $[RhCp^*(diimine)H_2O]^{2+}$ moiety inside the photochemical NADH regeneration system.[45−48]

Separation of the products and the regenerating catalyst for photoenzymatic processes was found to be an unsolved issue. As the rhodium catalyst is the costly part of most described regioselective photochemical regeneration methods for NADH, it would be beneficial to separate and reuse the hydride-transfer catalyst also in photochemical systems. Furthermore, $[RhCp^*(bpy)H_2O]^{2+}$ can inactivate certain redox enzymes[49] that are used to reduce various substrates of interest. This can be the case for CO_2 reduction with formate dehydrogenase[44,48] and for numerous more specialized and stereoselective enzymatic

dx.doi.org/10.1021/ja506060u | J. Am. Chem. Soc. 2014, 136, 12721−12729

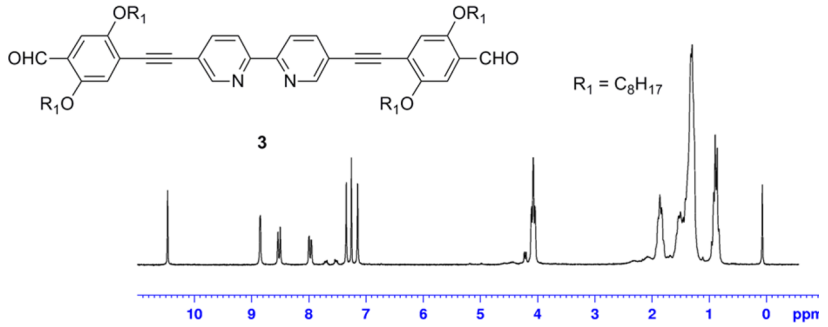

Figure 2. ^{1}H NMR scan (200 MHz, $CDCl_3$) of compound **3**.

reactions.[8] In Figure 1, a general scheme for such photoenzymatic systems is shown.

In the present work, a new bipyridine-containing poly(arylene-ethynylene)-*alt*-poly(arylene-vinylene) copolymer with a redox-active rhodium cyclopentadienyl complex as the active site for catalytic substrate conversion is presented. Its application for the chemoenzymatic and photochemical regeneration of NADH is introduced and described in detail. When transferred on solid substrates, such as glass beads, this active polymer-based hydride-transfer catalyst can be easily separated from the reaction solution and furthermore be used repeatedly under different aqueous reaction conditions because of its high stability. The polymer compound reduces redox cofactors with triethanolamine (TEOA) as electron donor. It works as both immobilizing agent and photosensitizer and thus, in contrast to similar systems with free rhodium complexes in solution, could minimize the contact of the catalyst compound with the NADH-binding site of enzymes applied in photoenzymatic redox systems.

RESULTS AND DISCUSSION

Synthesis and Characterization of the Polymer. A prerequisite for obtaining the polymer-based rhodium complex **Rh-BipyE-PV*ab*** is the prior synthesis of the metal-free polymer **BipyE-PV*ab***, as depicted in Scheme 1. 5,5′-Bis(4-formyl-2,5-dioctyloxyphenylethynyl)-2,2′-bipyridine (**3**) was obtained in ∼55% yield through Sonogashira Pd-catalyzed cross-coupling reaction of 4-formyl-2,5-dioctyloxyphenylacetylene (**1**) with 5,5′-dibromo-2,2′-bipyridine (**2**) and chromatographic workup. Figure 2 depicts the ^{1}H NMR spectrum of compound **3**.

All peaks can be readily assigned to the expected chemical structure. The subsequent Horner−Wadsworth−Emmons olefination reaction of **3** with 2,5-bis(2-ethylhexyloxy)-*p*-xylylene-bis(diethylphosphonate) (**4**) using potassium *tert*-butoxide in excess as base led to the desired polymer. **BipyE-PV*ab*** was obtained as a red product in 84% yield after Soxhlet extraction of the crude polymer with a refluxing methanol/diethyl ether mixture. The combination of linear octyl- and branched 2-ethylhexyloxy side chains enables good solubility in common organic solvents and good film-forming ability. The chemical structure of **BipyE-PV*ab*** was confirmed by ^{1}H and ^{13}C NMR spectroscopy. The broadness of the ^{1}H NMR peaks is a clear indication for the polymeric nature of the material. Size exclusion chromatography was used to estimate the polymer characteristics. Calibrated with polystyrene standards, it provided a number-average molecular weight, M_n, of 10 900 g mol^{-1} and a weight-average molecular weight, M_w, of 38 500 g mol^{-1}, leading to a polydispersity index, PDI,[50] of 3.5 and an average degree of polymerization, P_n, of 9.

The newly synthesized materials were designed to work as light-harvesting photosensitizers in the presence of substrate-containing solvents. Therefore, at first the photophysical characterization was performed in solution, and the maxima of absorption (λ_a) and emission (λ_f), as well as fluorescence quantum yield (Φ_f) values were determined. The results of these measurements are summarized in Table 1. The UV−vis

Table 1. Optical Absorption (λ_a)/Emission (λ_f) Maxima and Fluorescence Quantum Yield (Φ_f) Data of the Investigated Compounds in Chloroform Solution

compound	λ_a/nm	λ_f/nm	Φ_f	$\lambda_{exc.}$/nm
3	351, 402	443	0.5[a]	402
			0.44[a]	351
BipyE-PV*ab*	336, 459	526	0.49[a]	347
			0.56[b]	
Rh-BipyE-PV*ab*	360, 491	weak	weak	

[a]Standard: quinine sulfate in 0.1 M H_2SO_4. [b]Standard: sodium fluorescein.

spectrum of **BipyE-PV*ab*** shows a strong red shift due to higher conjugation length compared to the initial bipyridyl-containing dialdehyde **3**. A further red shift occurs after complexation with rhodium at the bipyridyl moiety upon formation of **Rh-BipyE-PV*ab***, which has also been reported for the corresponding monomeric rhodium(III) complexes of such 5,5′-bis(phenylethynyl)-2,2′-bipyridine ligands.[24]

The dialdehyde **3** shows two distinct absorption maxima at 351 and 402 nm. The luminescence maximum lies at 443 nm, with a quantum yield of Φ = 0.5 (excitation at 402 nm, calibration against quinine sulfate). It is important to note that the intensity of the blue luminescence usually observed for this class of polypyridyl derivatives at room temperature in solution is known to be very sensitive to slight pH variations and solvent purity effects.[24,51] In chloroform solution, the polymeric bipyridine-containing material **BipyE-PV*ab*** also shows two main absorption bands, with peaks at 336 and 491 nm. Upon excitation at 347 nm, the emitted light shows maximum intensity at 526 nm. Using two different luminescence standards (quinine sulfate and sodium fluorescein), a quantum yield of Φ = 0.50 ± 0.05 was obtained. The blue-green luminescence of the polymer **BipyE-PV*ab***, with a maximum around 526 nm, is almost completely quenched upon complexation of the polymer with rhodium to give **Rh-BipyE-PV*ab***. Such behavior was also found in earlier studies with the corresponding monomeric model substances.[24] The metal-containing polymer **Rh-BipyE-PV*ab*** shows only very weak background emission. This is tentatively ascribed to the

dx.doi.org/10.1021/ja506060u | J. Am. Chem. Soc. 2014, 136, 12721−12729

remaining nonmetalated polypyridyl sites in the material. Additionally, the optical absorbance is significantly red-shifted by about 50 nm compared to that of the parent polymer upon metalation of the bipyridine moiety. Optical absorption and emission spectra of the **BipyE-PV*ab*** polymer and the **Rh-BipyE-PV*ab*** system in chloroform are shown in Figure 3.

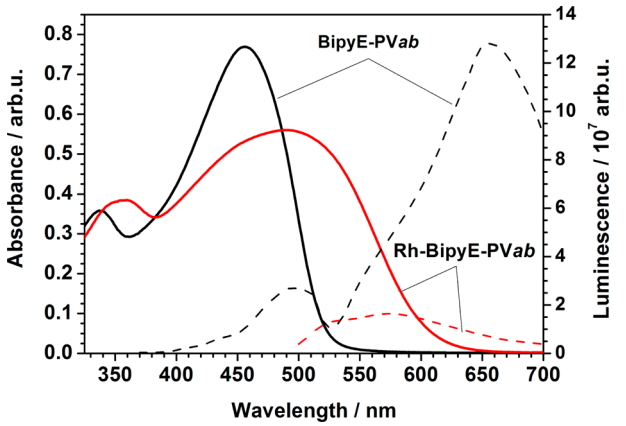

Figure 3. Absorption (solid lines) and emission spectra (dashed lines) of **BipyE-PV*ab*** and **Rh-BipyE-PV*ab*** (Rh-polymer) in spectroscopic dichloromethane; the optical absorbance of the initial bipyridyl polymer **BipyE-PV*ab*** in chloroform is red-shifted upon complex formation with rhodium by about 50 nm. The emission of **BipyE-PV*ab***, with a maximum at 657 nm, is quenched upon complexation of the bipyridyl moiety. The **Rh-BipyE-PV*ab*** polymer shows a weak emission, with a maximum at 571 nm.

Ellipsometry of the Polymer. The optical properties of the **BipyE-PV*ab*** polymer as a thin film were determined using spectroscopic ellipsometry (SE). Using this technique, information about the material's dielectric function was obtained. Measured SE ψ and Δ functions were fitted using the three oscillator model, and the values of the real and imaginary part of the dielectric function were obtained.[52,53] The resulting plots are presented in Figure 4. For better visibility of the absorption features, the energy scale in the graph was kept in eV. The plot of the imaginary part (in black), which describes the absorption of the material, shows two main absorption maxima at 460 nm (2.7 eV) and 348 nm (3.5 eV), respectively. An additional broad absorption band can be found at 218 nm (5.7 eV). The plotted absorptions are connected with the oscillations, which are described by the real part of the dielectric function. For all described absorption peaks, the related oscillators could be found and are Kramers–Kronig consistent. The optical band gap of the film material was found to be 590 nm (2.1 eV). The solid-state absorption features of the material determined by this method, with maxima at 348 and 460 nm, are relatively similar to the data measured for the nonmetalated polymer **BipyE-PV*ab*** in chloroform solution, where maxima were found at 336 and 459 nm, respectively.

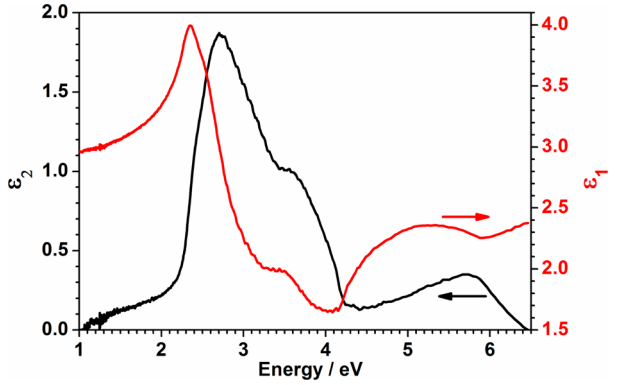

Figure 4. Ellipsometric characterization of **BipyE-PV*ab***. The calculated real part (plotted in red) and the imaginary part (plotted in black) of the dielectric function.

Chemical Doping of the Polymer with Iodine. To characterize the effects of possible redox processes involving the polymer backbone, a detailed characterization using ATR-FTIR was performed. Upon chemical oxidation with iodine, positively charged defects (holes) are formed within the polymer chain. Due to this oxidation (doping) process, the conductivity of the polymer increases and strong changes in the vibronic structure of the material occur, which can be monitored spectroscopically. In the present case, upon doping of the polymer with iodine, characteristic peaks of high oscillator strength arise in the FTIR spectrum of the material, which are connected with new infrared-active vibrational (IRAV) modes. Moreover, since the positive charge induces distortions in the polymer chain, a polaron band will be visible in the IR spectrum as a broad absorption feature. While the appearance of these new bands in the IR spectrum can be described by many theories,[54−58] in the present paper the Girlando–Painelli–Soos model was selected for further discussion.[59,60]

At first, the IR response of the pristine polymer **BipyE-PV*ab*** was measured. The resulting difference spectrum is presented in the Supporting Information (see Figure S1). The doping experiment was then performed during sequential IR measurements. These difference spectra are presented in Figure 5.

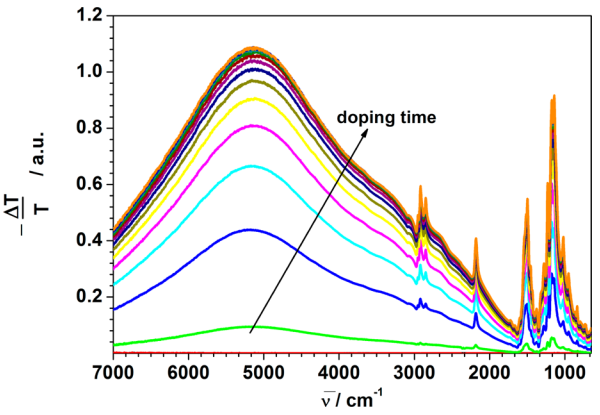

Figure 5. FTIR spectrum of the oxidative chemical doping of polymer **2** with iodine. When the material gets doped, two polaronic features appear at 5500 and 3500 cm^{-1} upon increasing degree of oxidation.

After doping, a broad absorption feature with a maximum at 5200 cm^{-1} appears, connected to the formation of the polaron. Together with the formation of the polaron, the appearance of new IRAV bands with maxima at 2100 and 1503 cm^{-1} as well as a broader peak at 1188 cm^{-1} can be observed. The presence of these bands suggests that, after doping, due to an increased distortion, previously symmetric vibrations became asymmetric and thus observable by IR.[54−58,61] Moreover, their rather high sharpness suggests that the free charge present in the polymer chain is rather localized.[59,60] Usually, such localization in a conjugated polymer suggests rather poor charge transport

dx.doi.org/10.1021/ja506060u | J. Am. Chem. Soc. 2014, 136, 12721−12729

properties.[59,60,62] However, for polymers containing a triple bond, the usual theories for conjugated polymers cannot directly describe the conducting properties of the polymer. Such polymers are usually characterized by strongly bound charges (between the triple bonds) that hinder intramolecular charge transport. On the other hand, the presence of this type of bonds can greatly improve the *inter*molecular charge transport (increase the film conductivity) due to the linear orientation of parts of the molecule.[63,64] Both the polaron absorption at 5200 cm^{-1} and the IRAV bands at lower energy show stronger intensity only with increasing doping level, and no significant shift of the bands themselves can be observed, which was also found to be the case when other triple-bond-containing polymers were studied.[64]

Electrochemical and Photoelectrochemical Characterization of the Polymer. The electrochemistry of the **BipyE-PV*ab*** polymer was investigated in order to obtain more detailed information about the redox properties of the system. As the total amount of sample was quite small, the oxidation of **BipyE-PV*ab*** was characterized using photoelectrochemical scanning droplet cell microscopy, which allows us to perform a full electrochemical characterization using small amounts of the studied material. Due to the slow kinetics of the electrochemical process monitored, the measurement was performed with a polarization speed of 1 mV s^{-1}. The resulting curve is presented in Figure 6a.

As can be seen, for potentials up to 1.10 V vs SHE (standard hydrogen electrode), no electrochemical processes occur, and only a background current can be measured. Above 1.10 V vs SHE, an increase in the current density can be noticed with a maximum at 1.22 V vs SHE. This increase is a result of the electrochemical oxidation of the **BipyE-PV*ab*** polymer. At higher potentials (above 1.3 V vs SHE), an additional increase in the current density can be observed. However, the nature of this current density increase is mostly connected with degradation of the electrochemical system.[65,66] Measuring in the backward direction, only background current was measured, suggesting the irreversibility of the electrochemical oxidation process. Since the polymer was developed to serve as a photosensitizer, additional photoelectrochemical characterization was performed. In this measurement, the polymer layer was kept at constant potential of 0 V vs SHE, and the change in the current upon illumination was measured. The sample was illuminated with a laser diode (532 nm, 153 mW cm^{-2}) fitting to the absorbance maximum of the polymer (as presented in Figure 4). The measurement was performed in 10 s dark/illumination sequences using a manually controlled shutter. The resulting curve is presented in Figure 6b. As can be noticed, during the first 10 s when the measurement was performed in the dark, only a background current could be measured in the range of nA cm^{-2}. After the sample was exposed to light, a strong change of the current was observed, originating from the photogeneration of separate charges. Within 10 s of illumination, a continuous decrease in current value can be observed, which results from shifted ground state and doped state absorption. After the shutter was closed, again only a background current could be measured. Further illumination sequences show a constant decrease of the photocurrent, which probably results from irreversible photooxidation of the investigated material. This photodegradation could also be enhanced by nonefficient charge extraction from the working electrode.

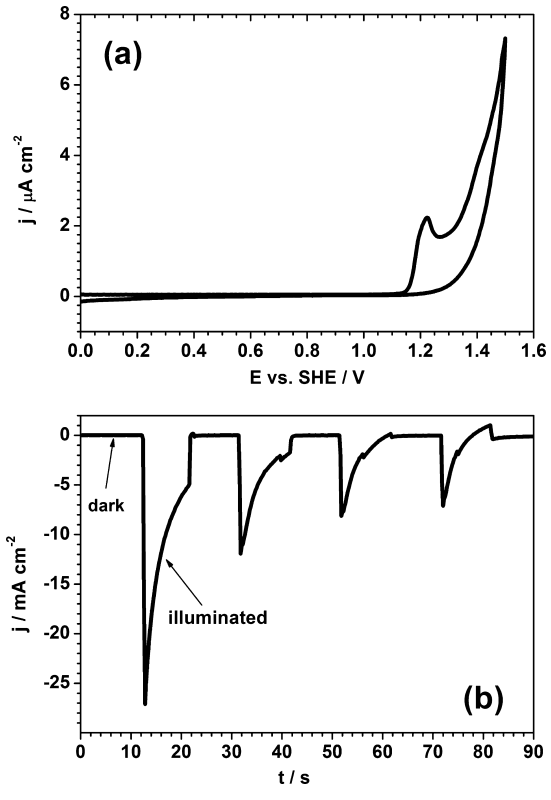

Figure 6. Electrochemical (a) and photoelectrochemical (b) characterization of the **BipyE-PV*ab*** polymer.

Chemical Catalysis: Reduction of NAD^+ with Formate on Rh-Polymer-Coated Glass Beads. In order to show that the rhodium site of the metalated polymer material **Rh-BipyE-PV*ab*** is accessible for the NAD^+ substrate and active in aqueous solution, catalyzed chemical reduction of NAD^+ to NADH in the presence of sodium formate was performed. The related rhodium 2,2′-bipyridyl complex [Rh(bpy)Cp*Cl]Cl readily hydrolyzes once in contact with water, forming either the hydroxo or the aquo complex when the initial chloride ligand is lost. This latter equilibrium is dependent on the pH value of the solution.[9,35,67] The pH used in this study was around 7.4 for chemical reduction with formate and photoenzymatic reactions with glutamate dehydrogenase (GDH) and 8.9 for the photochemical reduction of NAD^+ using TEOA as a donor. The $[Rh(diimine)Cp^*H_2O]^{2+}$ derivative of **Rh-BipyE-PV*ab*** is assumed to be the actual species in the former and $[Rh(diimine)Cp^*(OH)]^+$ in the latter case, as the pK_a of the water bound to the rhodium metal center of $[Rh(bpy)Cp^*H_2O]^{2+}$ used for comparison is around 8.2.[34]

Clean simple glass beads (diameter: 5 mm) were coated with **Rh-BipyE-PV*ab*** by mixing them into a solution of **Rh-BipyE-PV*ab*** in dichloromethane and leaving them to dry. The beads were transferred to an aqueous buffer solution containing both NAD^+ and sodium formate. The reaction solution was purged with Ar. The setup and the reaction scheme for this experiment are shown in Figure 7. Formate can donate H^- [68] to the rhodium reaction center, resulting in formation of CO_2 gas as an easily removable side product.[10] The formation of NADH due to the catalyzed chemical reduction of NAD^+ in this dark experiment was followed by recording UV−vis spectra of the sample solution at regular time intervals of 2 h (Figure 8).

Formation of the reduction product NADH was further confirmed via measurement of the fluorescence spectrum of the

dx.doi.org/10.1021/ja506060u | J. Am. Chem. Soc. 2014, 136, 12721−12729

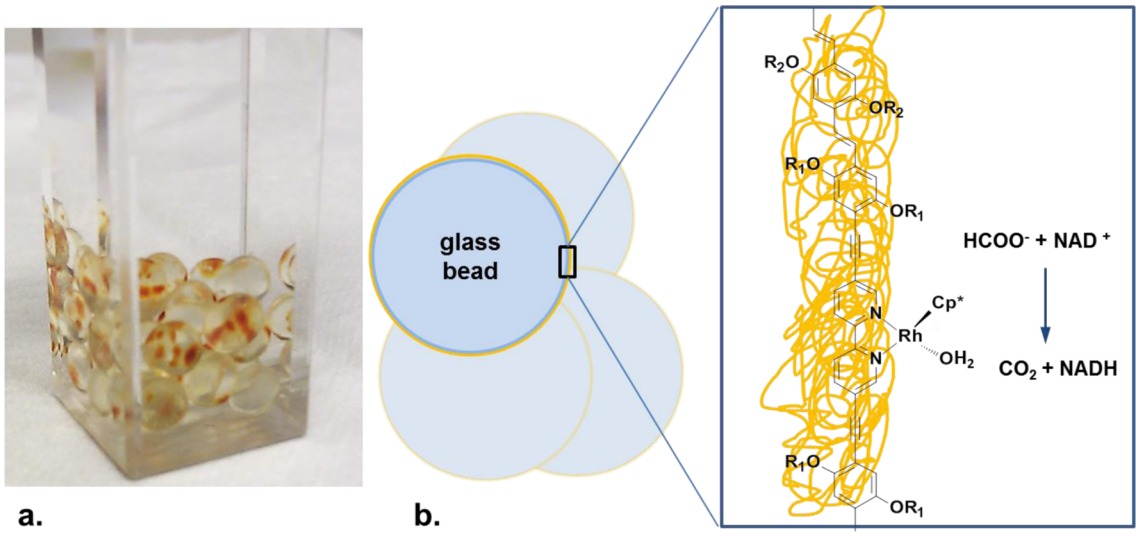

Figure 7. (a) Experimental setup. (b) Scheme of the surface reaction in the chemical reduction of NAD^+ to NADH with sodium formate as hydride donor to the polymer-bound rhodium catalyst reaction center.

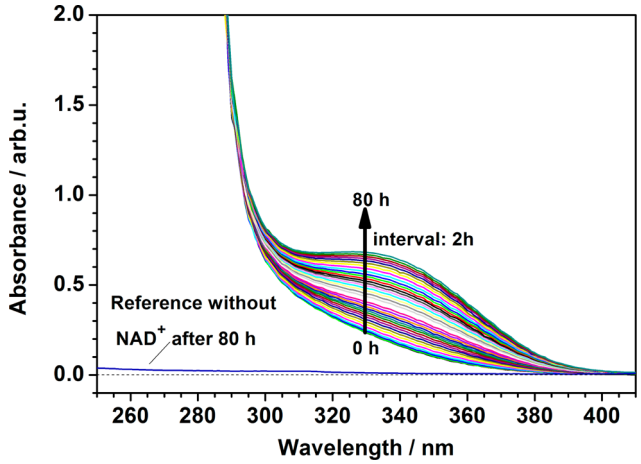

Figure 8. UV−vis spectra of the chemical reduction of NAD^+ with formate. The formation of NADH can be observed with increasing absorbance at 340 nm. Spectra were recorded at regular time intervals of 2 h for a total time of 80 h. The reaction solution was not stirred. No formation of a similar absorbance band could be observed in the reference sample without NAD^+.

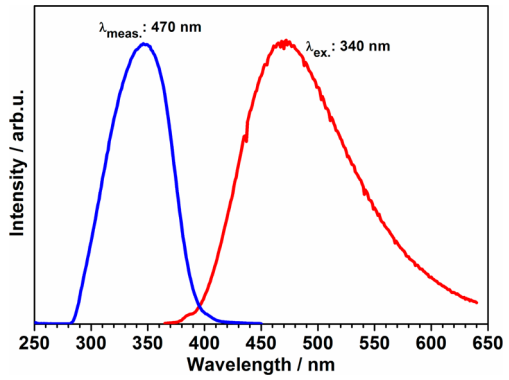

Figure 9. Luminescence and optical excitation spectrum of a dark sample containing the Rh-polymer beads and NAD^+ after 80 h of reaction without stirring. The specific luminescence with a maximum at 470 nm upon excitation with a wavelength of 340 nm indicates the formation of NADH.

sample, as can be seen in Figure 9. Upon excitation of the sample at 340 nm, the luminescence spectrum of the NADH formed in the solution had a maximum at 470 nm. The excitation spectrum recorded at 470 nm showed a maximum at 340 nm. Both these value are well in accordance with literature data on the reduced cofactor NADH.[69] The experiment was also repeated with the same batch of **Rh-BipyE-PV*ab***-coated beads after they were rinsed with distilled water and put into a fresh solution containing NAD^+ and formate.

Photocatalysis: Reduction of NAD^+ with Triethanolamine on Rh-Polymer-Coated Glass Beads. To investigate the applicability of the synthesized rhodium polymer further, a photolysis experiment was performed. TEOA was used as a sacrificial donor in a 0.1 M aqueous buffered sodium phosphate solution to enhance the stability of both the NAD^+ and the NADH present in the sample, which was necessary due to the relatively long irradiation time.[70] One advantage of the system used here is the fact that the UV−vis spectrum of the solution can be measured separately from the that of the photocatalyst, as the cuvette was not completely filled with the catalyst-coated glass beads (similar to the reaction depicted in Figure 7). This makes the detection of the 340 nm absorbance band of NADH straightforward. **Rh-BipyE-PV*ab***-coated glass beads were used in an experiment with 3 mL solution of 15 w/v% TEOA in 0.1 M sodium phosphate buffer with a pH value of 8.9, and 1.2 mg of NAD^+, stirred and irradiated at $\lambda \geq 390$ nm for 26 h. The UV−vis spectra recorded can be seen in Figure 10. Blue lines show the UV−vis absorbance and emission data of the dark sample; similar data for the irradiated sample are shown in red. After 26 h, no spectral changes occurred in the dark sample, whereas for the sample that had been irradiated at $\lambda \geq 390$ nm, a distinct absorbance band with a maximum at 340 nm was formed, which indicates the successful photocatalytic formation of NADH catalyzed by the **Rh-BipyE-PV*ab*** polymer. Additionally, the sample was also investigated by emission spectroscopy. The reduction product NADH was further confirmed by measuring the fluorescence spectrum (Figure 10) of the sample upon excitation at 340 nm, and the excitation spectrum was recorded at 470 nm.[12,69] The amount of product formed in the photocatalytic system was estimated from the

dx.doi.org/10.1021/ja506060u | J. Am. Chem. Soc. 2014, 136, 12721−12729

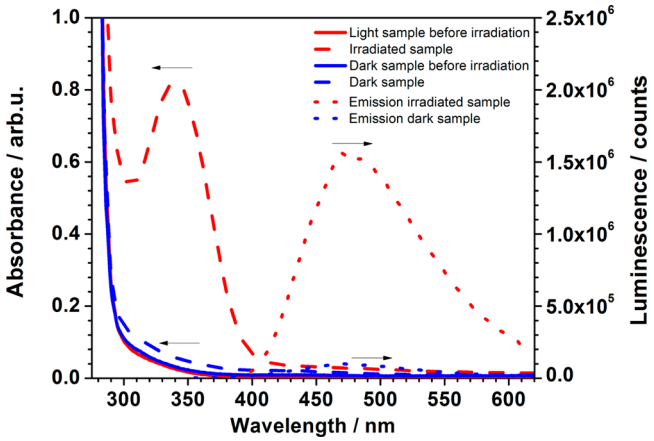

Figure 10. UV–vis absorption and emission spectrum of an irradiated sample ($\lambda \geq 390$ nm) with **Rh-BipyE-PV*ab*** glass beads, 15 w/v% TEOA as sacrificial donor, and NAD^+ as substrate. After 26 h, an increased absorbance at 340 nm indicates the photochemical formation of NADH. Photoluminescence measurements of the sample with λ_{exc}: 340 nm also indicates the successful synthesis of NADH, which shows a specific emission at 470 nm; after 26 h, the conversion of NADH was estimated to be 21%, compared to the initial amount of NAD^+ added from the UV–vis spectrum applying Lambert–Beer's law (ε = 6300 cm^{-1} mol^{-1} L).[69]

difference in UV–vis absorbance maximum at 340 nm applying Lambert–Beers law with ε = 6300 cm^{-1} mol^{-1} L for the reduction product NADH.[69] The conversion to NADH after 26 h compared to the initial amount of NAD^+ was more than 21% (8.6 mg NADH l^{-1}). This results, using the surface area of the glass beads, in a turnover number (TON) of 480 μmol cm^{-2} and a turnover frequency (TOF) of 1.8 μmol cm^{-2} h^{-1}. The **Rh-BipyE-PV*ab*** polymer-coated glass beads were used in a second photolysis experiment after being rinsed carefully with ultrapure water. In a solution with pH 8, the quantum yield of the Rh-polymer film was measured to be 1.0×10^{-4} ($\pm$ 0.1×10^{-4}) when using a 370 nm low-pass filter. It was calculated according to the formula applied in the literature[46] as the ratio between 2 times the amount of NADH formed and the amount of absorbed photons. The amount of photons absorbed by the **Rh-BipyE-PV*ab*** film was obtained by integration of the difference in transmitted light through the sample with and without a polymer film drop-cast on the inside of the cuvette over the spectral range up to 650 nm, which is the low-energy absorbance edge of **Rh-BipyE-PV*ab*** (see Figure 3).

Photoenzymatic Catalysis: Reduction of α-Ketoglutarate by Glutamate Dehydrogenase Using the NADH Formed in the Photolysis as Redox Cofactor. In order to show that the NADH formed by the photoreaction of NAD^+ on **Rh-BipyE-PV*ab*** is enzymatically active, enzymatic reduction of α-ketoglutarate to L-glutamate was coupled to the photochemical regeneration system described before. Optimized conditions for the performance of GDH type 1 from bovine liver were applied, similar to described literature procedures.[28,29,45] **Rh-BipyE-PV*ab*** (0.08 mg) was drop-cast from dichloromethane solution on a simple glass sheet. The glass substrate was used in a quartz cuvette for the irradiation experiment. The reaction buffer (pH 7.4) containing 0.1 M phosphate, 0.1 M ammonium sulfite, and 15 w/v% TEOA with 0.7 mM NAD^+, 13 mM α-ketoglutarate, and 5 U GDH was first stirred in the dark for 1 h.[45] After 5 h of irradiation with a 370 nm cutoff filter and after 22 h of irradiation, 6.9 and 24.3 ppm of L-glutamic acid were detected, respectively, in the photolysis solution by HPLC-MS. No L-glutamic acid was detected after the solution was stirred without light irradiation.

CONCLUSIONS

The luminescence of the **BipyE-PV*ab*** polymer is almost completely quenched after complexation with the rhodium metal (to form **Rh-BipyE-PV*ab***). This indicates efficient interaction between the polymer backbone and the Rh subunits. The catalytically active sites—the rhodium metal centers of the polymer—have been shown to be readily accessible to both a hydride donor and the NADH substrate, making the polymer applicable in the catalyzed chemical NAD^+ reduction with formate as a hydride source. The polymer material can also be applied in a photocatalytic system with TEOA as electron donor. Concerning the mechanism of this photoreaction, there are several different possibilities, which at the present stage of our investigations cannot be fully distinguished. Moreover, the question of how such a polymer works as a photocatalyst for NAD^+ hydrogenation cannot be described with a classical theory about molecular catalysis alone. As the iodine doping experiments show, the **BipyE-PV*ab*** material is dopable to become a p-type organic semiconductor, and thus it can also show electrical conductivity. The polymer does not behave completely like a conjugated conducting polymer because the triple bond structure favors intermolecular conductivity over intramolecular conductivity. Thus, the theoretical concepts for (conducting) polymer chemistry, as applied in organic electronics with a classical moving polaron approach, cannot be used to describe the system. Classical

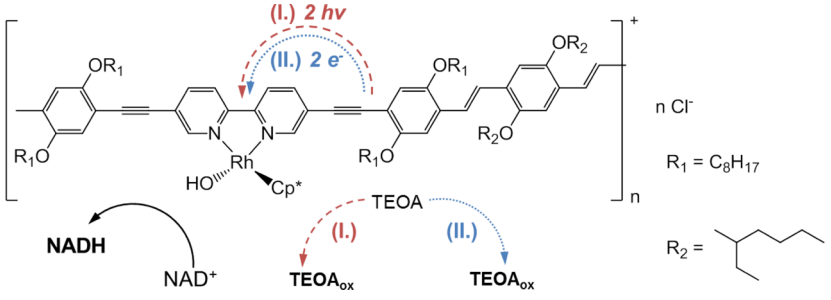

Figure 11. Schematic representation of two possible catalytic pathways proposed for the photochemical reduction of NAD^+ to NADH by the rhodium polymer **Rh-BipyE-PV*ab***: (I) The donor TEOA reductively quenches the excited state of the Rh-complex. This would have to happen twice before a hydride can be formed by protonation and then be transferred to NAD^+. (II) The rhodium complex oxidatively quenches the excited state of the polymer backbone material **BipyE-PV*ab***, which is regenerated by TEOA from the aqueous solution.

dx.doi.org/10.1021/ja506060u | J. Am. Chem. Soc. 2014, 136, 12721–12729

photochemistry, as it would be assumed to take place in dilute solution, does not seem to be sufficient either.

The two most probable catalytic pathways tentatively proposed for the reaction are shown in Figure 11. The first possibility (I) would involve direct excitation of the rhodium subunit or energy transfer from the irradiated polymer **BipyE-PV*ab*** to the Rh center in **Rh-BipyE-PV*ab*** and reductive quenching of the excited state by TEOA. This would have to occur twice at the same Rh site for later reduction of NAD^+ to NADH.

The second possible pathway (II) involves (oxidative) quenching of the photoexcited polymer chain by a rhodium center. This is accompanied by electron transfer to the rhodium active site, possibly also involving a different polymer chain. Especially considering the facts that iodine vapor, with an estimated redox potential of 0.35 ± 0.1 V,[71] is sufficient to oxidize the **BipyE-PV*ab*** polymer backbone and the bandgap measured by ellipsometry is 2.1 eV, this pathway is the more probable one. The ground state of the polymer chain is presumably recovered by TEOA as a sacrificial electron donor. After two electron-transfer steps to the rhodium center, a proton can be taken up from the solution, and the active Rh-hydride complex is formed at the active bipyridyl coordination site of the rhodium polymer. The hydride is then transferred regioselectively to the additionally coordinated NAD^+ to form 1,4-NADH.[9,10,36−38,49]

The amount of L-glutamate formed per repetition unit of the **Rh-BipyE-PV*ab*** polymer (M = 1560 g mol^{-1}) can be used to roughly estimate a TON per rhodium center of 3.2 (after 22 h). However, as this is a surface reaction on a randomly drop-cast film, it is most likely the case that not all rhodium centers that are stoichiometrically present in the structure are similarly accessible to drive the photoreaction. Thus, this TON is likely an underestimation. Nevertheless, it shows that the NADH regeneration in the enzymatically coupled photoreaction is catalytic with respect to the **Rh-BipyE-PV*ab*** polymer photosensitizer. The TOF for **Rh-BipyE-PV*ab*** is 0.145 h^{-1}, comparable to those of other reported systems applying heterogeneous photosensitizers (CdSe, 0.168 h^{-1}; CdS, 0.120 h^{-1}; p-doped TiO_2, 0.003 h^{-1}; and $W_2Fe_4Ta_2O_{17}$, 0.002 h^{-1}.[29]

The photochemical quantum yield, 1.0×10^{-4} ($\pm$ 0.1×10^{-4}), and the amount of NADH formed per unit area and time, 1.8 μmol cm^{-2} h^{-1}, are comparable measures for this heterogeneous polymer−catalyst system.

The **Rh-BipyE-PV*ab*** polymer can be used as very stable, separable, and reusable photocatalyst for visible-light-powered cofactor reduction with electron donors present in the solution as well as for chemical cofactor reduction with hydride donor molecules such as formate. The precious component of the otherwise very effective rhodium systems for NADH regeneration can be separated and reused in different experimental environments, and interference with the following reactions as well as possible deactivation of the active side of redox-active enzymes which are coupled to the system by soluble redox mediators can be minimized.[49] The concept probably can be extended to photoelectrochemical pathways of NAD^+ reduction by modification of the polymer backbone to enhance intramolecular charge carrier mobility. The polymers could be modified to provide more active sites per repetition unit, and the optical properties of the polymer can be tuned by using different copolymerization agents. Investigations in this direction are currently underway in our group.

A method for more uniform film formation on the glass substrates has to be found, and the use and investigation of the catalytic film on glass substrates are areas of interest for upcoming research. Further work on electrocatalysis and photoelectrocatalysis using this conjugated polymer is also underway.

■ ASSOCIATED CONTENT

Supporting Information

Polymer materials' synthesis and characterization, especially IR spectrum of the pristine polymer material, **BipyE-PV*ab***; NMR scans of compound **3**, **BipyE-PV*ab***, and **Rh-BipyE-PV*ab***; cyclic voltammogram of **Rh-BipyE-PV*ab***; and description of spectroscopic, spectrometric, and electrochemical measurements' methods and instrumentation. This material is available free of charge via the Internet at http://pubs.acs.org.

■ AUTHOR INFORMATION

Corresponding Author

kerstin.oppelt@jku.at

Notes

The authors declare no competing financial interest.

■ ACKNOWLEDGMENTS

This research was supported by Solar Fuel GmbH and the Austrian Science Fund (FWF project P21045: "Bio-inspired Multielectron Transfer Photosensitizers"). NMR-facility funding from the European Union through the EFRE INTERREG IV ETC-AT-CZ program (project M00146, "RERI-uasb") is gratefully acknowledged. G.K. also thanks the German Research Foundation (DFG GRK1626 "Chemical Photocatalysis") and the European Commission (COST action CM1202 "Supramolecular Photocatalytic Water Splitting") for partial support of this work. We thank Eckhart Birckner from Friedrich-Schiller University of Jena for performing the luminescence quantum yield measurements.

■ REFERENCES

(1) Knör, G. *Chem.—Eur. J.* **2009**, *15*, 568.
(2) Kim, J. H.; Nam, D. H.; Park, C. B. *Curr. Opin. Biotechnol.* **2014**, *28*, 1.
(3) Sakai, T.; Mersch, D.; Reisner, E. *Angew. Chem., Int. Ed.* **2013**, *52*, 12313.
(4) Dibenedetto, A.; Stufano, P.; Nocito, F.; Aresta, M. *ChemSusChem* **2011**, *4*, 1311.
(5) Aresta, M.; Dibenedetto, A.; Angelini, A. In *Comprehensive Inorganic Chemistry II*; Reedijk, J., Poeppelmeier, K. B. T., Eds.; Elsevier: Amsterdam, 2013; Vol. *6*, pp 563−586.
(6) Dibenedetto, A.; Stufano, P.; Macyk, W.; Baran, T.; Fragale, C.; Costa, M.; Aresta, M. *ChemSusChem* **2012**, *5*, 373.
(7) Aresta, M.; Dibenedetto, A.; Angelini, A. *J. CO2 Util.* **2013**, *3−4*, 65.
(8) Hollmann, F.; Arends, I. W. C. E.; Buehler, K. *ChemCatChem* **2010**, *2*, 762.
(9) Grau, M. M.; Poizat, M.; Arends, I. W. C. E.; Hollmann, F. *Appl. Organomet. Chem.* **2010**, *24*, 380.
(10) Hollmann, F.; Witholt, B.; Schmid, A. *J. Mol. Catal. B Enzymol.* **2003**, *19−20*, 167.
(11) Hollmann, F.; Hofstetter, K.; Schmid, A. *Trends Biotechnol.* **2006**, *24*, 163.
(12) Oppelt, K. T.; Wöß, E.; Stiftinger, M.; Schöfberger, W.; Buchberger, W.; Knör, G. *Inorg. Chem.* **2013**, *52*, 11910.
(13) Obert, R.; Dave, B. C. *J. Am. Chem. Soc.* **1999**, *121*, 12192.

(14) Olah, G. A.; Goeppert, A.; Surya Prakash, G. K. *Beyond Oil and Gas: The Methanol Economy*, 2nd ed.; Wiley-VCH Verlag GmbH & Co. KGaA: Weinheim, 2009.
(15) Portenkirchner, E.; Oppelt, K.; Egbe, D. A. M.; Knör, G.; Sariciftci, N. S. *Nanomater. Energy* **2013**, *2*, 134.
(16) Knör, G.; Monkowius, U. *Adv. Inorg. Chem.* **2011**, *63*, 235.
(17) Egbe, D. A. M.; Ulbricht, C.; Orgis, T.; Carbonnier, B.; Kietzke, T.; Peip, M.; Metzner, M.; Gericke, M.; Birckner, E.; Pakula, T.; Neher, D.; Grummt, U.-W. *Chem. Mater.* **2005**, *17*, 6022.
(18) Birckner, E.; Grummt, U. U.-W.; Göller, A. H.; Pautzsch, T.; Egbe, D. A. M.; Al-Higari, M.; Klemm, E. *J. Phys. Chem. A* **2001**, *105*, 10307.
(19) Egbe, D. A. M.; Roll, C. P.; Birckner, E.; Grummt, U.-W.; Stockmann, R.; Klemm, E. *Macromolecules* **2002**, *35*, 3825.
(20) Liu, Y.; Li, Y.; Schanze, K. S. *J. Photochem. Photobiol. C Photochem. Rev.* **2002**, *3*, 1.
(21) Walters, K. A.; Premvardhan, L. L.; Liu, Y.; Peteanu, L. A.; Schanze, K. S. *Chem. Phys. Lett.* **2001**, *339*, 255.
(22) Egbe, D. A. M.; Cornelia, B.; Nowotny, J.; Günther, W.; Klemm, E. *Macromolecules* **2003**, *36*, 5459.
(23) Egbe, D. A. M.; Bader, C.; Klemm, E.; Ding, L.; Karasz, F. E.; Grummt, U.-W.; Birckner, E. *Macromolecules* **2003**, *36*, 9303.
(24) Oppelt, K.; Egbe, D. A. M.; Monkowius, U.; List, M.; Zabel, M.; Sariciftci, N. S.; Knör, G. *J. Organomet. Chem.* **2011**, *696*, 2252.
(25) Lee, S. H.; Nam, D. H.; Kim, J. H.; Baeg, J.-O.; Park, C. B. *ChemBioChem* **2009**, *10*, 1621.
(26) Song, H.-K.; Lee, S. H.; Won, K.; Park, J. H.; Kim, J. K.; Lee, H.; Moon, S.-J.; Kim, D. K.; Park, C. B. *Angew. Chem., Int. Ed.* **2008**, *47*, 1749.
(27) Lee, S. H.; Lee, H. J.; Won, K.; Park, C. B. *Chem.—Eur. J.* **2012**, *18*, 5490.
(28) Nam, D. H.; Park, C. B. *ChemBioChem* **2012**, *13*, 1278.
(29) Kim, J. H.; Lee, S. H.; Lee, J. S.; Lee, M.; Park, C. B. *Chem. Commun.* **2011**, *47*, 10227.
(30) Siu, E.; Won, K.; Park, C. B. *Biotechnol. Prog.* **2007**, *23*, 293.
(31) Lee, M.; Hong, J.; Seo, D.-H.; Nam, D. H.; Nam, K. T.; Kang, K.; Park, C. B. *Angew. Chem., Int. Ed.* **2013**, *52*, 8322.
(32) Lee, S. H.; Nam, D. H.; Park, C. B. *Adv. Synth. Catal.* **2009**, *351*, 2589.
(33) Steckhan, E. In *Electrochemistry V SE-3*; Steckhan, E., Ed.; Topics in Current Chemistry *170*; Springer: Berlin/Heidelberg, 1994; pp 83−111.
(34) Steckhan, E.; Herrmann, S.; Ruppert, R.; Dietz, E.; Frede, M.; Spika, E. *Organometallics* **1991**, *10*, 1568.
(35) Lo, H. C.; Buriez, O.; Kerr, J. B.; Fish, R. H. *Angew. Chem., Int. Ed.* **1999**, *38*, 1429.
(36) Lutz, J.; Hollmann, F.; Ho, T. V.; Schnyder, A.; Fish, R. H.; Schmid, A. *J. Organomet. Chem.* **2004**, *689*, 4783.
(37) Lo, H. C.; Fish, R. H. *Angew. Chem., Int. Ed.* **2002**, *41*, 478.
(38) Lo, H. C.; Leiva, C.; Buriez, O.; Kerr, J. B.; Olmstead, M. M.; Fish, R. H. *Inorg. Chem.* **2001**, *40*, 6705.
(39) Cosnier, S.; Gunther, H. *J. Electroanal. Chem. Interfacial Electrochem.* **1991**, *315*, 307.
(40) Cosnier, S.; Deronzier, A.; Moutet, J.-C. *J. Mol. Catal.* **1988**, *45*, 381.
(41) Kim, J. A.; Kim, S.; Lee, J.; Baeg, J.-O. *Inorg. Chem.* **2012**, *51*, 8057.
(42) Shi, Q.; Yang, D.; Jiang, Z.; Li, J. *J. Mol. Catal. B Enzymol.* **2006**, *43*, 44.
(43) Lee, S. H.; Ryu, J.; Nam, D. H.; Park, C. B. *Chem. Commun.* **2011**, *47*, 4643.
(44) Yadav, R. K.; Baeg, J.-O.; Oh, G. H.; Park, N.-J.; Kong, K.; Kim, J.; Hwang, D. W.; Biswas, S. K. *J. Am. Chem. Soc.* **2012**, *134*, 11455.
(45) Liu, J.; Huang, J.; Zhou, H.; Antonietti, M. *ACS Appl. Mater. Interfaces* **2014**, *6*, 8434.
(46) Liu, J.; Antonietti, M. *Energy Environ. Sci.* **2013**, *6*, 1486.
(47) Huang, J.; Antonietti, M.; Liu, J. *J. Mater. Chem. A* **2014**, *2*, 7686.
(48) Liu, J.; Cazelles, R.; Chen, Z. P.; Zhou, H.; Galarneau, A.; Antonietti, M. *Phys. Chem. Chem. Phys.* **2014**, *16*, 14699.
(49) Poizat, M.; Arends, I. W. C. E.; Hollmann, F. *J. Mol. Catal. B Enzym.* **2010**, *63*, 149.
(50) Stepto, R. F. T. *Pure Appl. Chem.* **2009**, *81*, 351.
(51) Kalyanasundaram, K. In *Photochemistry of Polypyridine and Porphyrin Complexes*; Kalyanasundaram, K., Ed.; Academic Press: London, 1992; pp 87−104.
(52) Gasiorowski, J.; Menon, R.; Hingerl, K.; Dachev, M.; Sariciftci, N. S. *Thin Solid Films* **2013**, *536*, 211.
(53) Gasiorowski, J.; Hingerl, K.; Menon, R.; Plach, T.; Neugebauer, H.; Wiesauer, K.; Yumusak, C.; Sariciftci, N. S. *J. Phys. Chem. C. Nanomater. Interfaces* **2013**, *117*, 22010.
(54) Horovitz, B. *Solid State Commun.* **1982**, *41*, 729.
(55) Ehrenfreund, E.; Vardeny, Z.; Brafman, O.; Horovitz, B. *Phys. Rev. B* **1987**, *36*, 1535.
(56) Zerbi, G.; Gussoni, M.; Castiglioni, C. In *Conjugated Polymers: The Novel Science and Technology of Highly Conducting and Nonlinear Optically Active Materials*; Brédas, J. L., Silbey, J., Eds.; Kluwer: New York, 1991; pp 435−507.
(57) Ehrenfreund, E. A.; Vardeny, Z. V. In *Proceedings of SPIE 3145, Optical Probes of Conjugated Polymers*; Vardeny, Z. V., Rothberg, L. J., Eds.; SPIE: San Diego, CA, 1997; pp 324−332.
(58) Lopez-Navarrete, J. T.; Tian, B.; Zerbi, G. *Solid State Commun.* **1990**, *74*, 199.
(59) Girlando, A.; Painelli, A.; Soos, Z. G. *J. Chem. Phys.* **1993**, *98*, 7459.
(60) Sariciftci, N. S.; Mehring, M.; Gaudl, K. U.; Bäuerle, P.; Neugebauer, H.; Neckel, A. *J. Chem. Phys.* **1992**, *96*, 7164.
(61) Del Zoppo, M.; Castiglioni, C.; Zuliani, P.; Zerbi, G. In *Handbook of Conducting Polymers*, 2nd ed.; Skotheim, T. A., Elsembaumer, R. L., Reynolds, J. R., Eds.; Marcel Dekker: New York, 1998; p 765ff.
(62) Gąsiorowski, J.; Głowacki, E. D.; Hajduk, B.; Siwy, M.; Chwastek-Ogierman, M.; Weszka, J.; Neugebauer, H.; Sariciftci, N. S. *J. Phys. Chem. C* **2013**, *117*, 2584.
(63) Garay, R. O.; Naarmann, H.; Muellen, K. *Macromolecules* **1994**, *27*, 1922.
(64) Gasiorowski, J.; Boudiba, S.; Hingerl, K.; Ulbricht, C.; Fattori, V.; Tinti, F.; Camaioni, N.; Menon, R.; Schlager, S.; Boudida, L.; Sariciftci, N. S.; Egbe, D. A. M. *J. Polym. Sci., Part B: Polym. Phys.* **2014**, *52*, 338.
(65) Gasiorowski, J.; Mardare, A. I.; Sariciftci, N. S.; Hassel, A. W. *J. Electroanal. Chem.* **2013**, *691*, 77.
(66) Gasiorowski, J.; Mardare, A. I.; Sariciftci, N. S.; Hassel, A. W. *Electrochim. Acta* **2013**, *113*, 834.
(67) Kölle, U.; Grätzel, M. *Angew. Chem.* **1987**, *99*, 572.
(68) Matsubara, Y.; Fujita, E.; Doherty, M. D.; Muckerman, J. T.; Creutz, C. *J. Am. Chem. Soc.* **2012**, *134*, 15743.
(69) Bisswanger, H. *Practical Enzymology*, 2nd ed.; Wiley-VCH Verlag & Co. KGaA: Weinheim, 2011.
(70) Chenault, H. K.; Whitesides, G. *Appl. Biochem. Biotechnol.* **1987**, *14*, 147.
(71) Boschloo, G.; Hagfeldt, A. *Acc. Chem. Res.* **2009**, *42*, 1819.